

Melittin at a membrane/water interface: Effects on water orientation and water penetration

Michal Bachar and Oren M. Becker

Citation: [The Journal of Chemical Physics](#) **111**, 8672 (1999); doi: 10.1063/1.480207

View online: <http://dx.doi.org/10.1063/1.480207>

View Table of Contents: <http://scitation.aip.org/content/aip/journal/jcp/111/18?ver=pdfcov>

Published by the [AIP Publishing](#)

Articles you may be interested in

[Sticky water surfaces: Helix-coil transitions suppressed in a cell-penetrating peptide at the air-water interface](#)
J. Chem. Phys. **141**, 22D517 (2014); 10.1063/1.4898711

[Inhomogeneity effects on the structure and dynamics of water at the surface of a membrane: A computer simulation study](#)
J. Chem. Phys. **126**, 125103 (2007); 10.1063/1.2715880

[Electrostatic interactions in a neutral model phospholipid bilayer by molecular dynamics simulations](#)
J. Chem. Phys. **116**, 3052 (2002); 10.1063/1.1436077

[Erratum: "An energy-based mapping method for identifying the in-plane orientations of polypeptides and other macromolecules at crystalline interfaces" \[J. Chem. Phys. 112, 5144 \(2000\)\]](#)
J. Chem. Phys. **113**, 2509 (2000); 10.1063/1.482072

[An energy-based mapping method for identifying the in-plane orientations of polypeptides and other macromolecules at crystalline interfaces](#)
J. Chem. Phys. **112**, 5144 (2000); 10.1063/1.481071



Melittin at a membrane/water interface: Effects on water orientation and water penetration

Michal Bachar and Oren M. Becker^{a)}

School of Chemistry, Tel Aviv University, Ramat Aviv, Tel Aviv 69978, Israel

(Received 11 December 1998; accepted 4 August 1999)

Melittin, a small peptide found in bee venom, is known to induce membrane lysis. A molecular dynamics simulation of melittin embedded in a hydrated dipalmitoylphosphatidylcholine bilayer is analyzed in order to study the peptide's effect on water molecules at the membrane/water interface. The peptide, with a protonated N-terminus, was embedded in a *trans*-bilayer orientation. The simulation highlights the microscopic mechanism by which melittin induces the formation of transmembrane water "pores," leading to membrane lysis. It was found that melittin has a profound effect on the behavior of the water molecules at the membrane/water interface. It modifies the orientation of the water dipoles and induces water penetration into the bilayer. In fact, melittin's residue Lys-7 and its protonated N-terminus facilitate the formation of transmembrane water pores by steering water penetration from both sides of the bilayer. The initial step towards pore formation takes about 200 ps, and the process relays on melittin's bent conformation and tilted orientation. A large body of experimental observations supports the simulation results and the suggested microscopic mechanism. © 1999 American Institute of Physics. [S0021-9606(99)50341-3]

I. BACKGROUND

Biological membranes play an important role in a large number of life's processes. While the overall structure of the membrane is determined by the lipid components, the interactions of lipids with the surrounding water molecules and with membrane-bound proteins are responsible for much of its diversity and function. Many processes are mediated through membrane-embedded proteins, such as receptors, ion channels, adhesion proteins, and pores. However, there are also many interesting membrane processes are directly related to the behavior of water near, at and inside the lipid membrane. Examples are water mediated interactions between two membranes (electrostatic shielding and the "hydration force"),¹ water permeation across the membrane which is of importance in maintaining the osmotic balance, and the formation of membrane-spanning water channels which mediate proton transfer. The orientation of water dipoles near the interface is thought to contribute to the electric field of the bilayer, affecting diffusion and permeation of small molecules.²

A molecular dynamics (MD) description of membrane/water and membrane/protein interfaces offers a detailed microscopic picture, unobtainable by experimental techniques, aiding in understanding many of these important phenomena.^{1,3} Methodological developments as well as increase in computer power have significantly advanced the ability to simulate complex biomembrane systems, with and without embedded peptides, in recent years. MD simulations of phospholipid bilayers began with modest model systems⁴ but have improved with time to the present level in which different types of solvated bilayers of more than 100 phos-

pholipids can be simulated.^{1,5-15} These simulations reproduce experimental results and probe, at an atomic level, the interactions between the bilayer and the surrounding water molecules.

The various MD studies have yielded important information about the behavior of water at the membrane interface. MD studies of phosphatidylcholine (PC) membranes (dimyristoyl-phosphatidylcholine DMPC and dipalmitoyl-phosphatidylcholine DPPC) showed that the lipids significantly influence water out to several hydration shells.^{3,16,17} A preferential ordering of water molecules at the membrane-water interface was observed. Far from the lipid/water interface water molecules are randomly oriented with respect to the plane of the membrane (the average angle between the water dipoles and the membrane normal is 90°). However, in the vicinity of the headgroups, within the lipid/water interface, water molecules are oriented in such a way that the positive end of the water dipole points on average towards the bilayer interior. In DPPC the average angle of the water dipoles to the surface normal at this region was found to be about 110°–115°.¹⁶ Thus the lipid headgroups induce orientational order in the neighboring water molecules, which in the DPPC interface compensates for the P–N dipole of the headgroups. In the case of large dipolar fields, such as those present at the PC membranes, the main ordering effect of the water molecules originates from the local electrostatic charge distribution (and not by the tendency to form hydrogen bonds).¹⁷ The presence of large dipolar charges on the lipid headgroups is also the reason for the broad interface region observed. A similar ordering of the water dipoles at the membrane/water interface was found in an MD simulations of dilauroyl-phosphatidylethanolamine (DLPE) which has a dipolar head group similar to PC.¹⁸ One hypothesis, recently supported by experiment, links the positive membrane "di-

^{a)}Author to whom correspondence should be addressed; electronic mail: becker@sapphire.tau.ac.il

pole'' potential to the preferential ordering of water molecules at the membrane water interface.^{2,19}

The characterization of membrane/water interfaces becomes more complex in the presence of membrane-bound or membrane-embedded proteins. In the last few years, several research groups have begun performing detailed MD simulations of phospholipid bilayer with bound or embedded peptides.^{1,20–27} These efforts culminated in an unprecedented large simulation, consisting of a porin trimer in a hydrated 318 POPE phospholipids bilayer, performed by Tieleman and Berendsen.²⁸ Most of these simulations focused on the affect of the membrane on the embedded protein, although the complementary effect of the embedded protein on the lipids was addressed whenever possible.

A common model for a membrane/protein system, which is also of specific biophysical interest, consists of the peptide melittin bound to a phospholipid bilayer. Melittin is the principal toxic component in the honeybee venom, responsible for lysis of the cell membrane.^{29,30} This cationic peptide consists of the 26 amino acid sequence Gly-Ile-Gly-Ala-Val⁵-Leu-Lys-Val-Leu-Thr¹⁰-Thr-Gly-Leu-Pro-Ala¹⁵-Leu-Ile-Ser-Trp-Ile²⁰-Lys-Arg-Lys-Arg-Gln²⁵-Gln. The 20 amino acids at the N-terminus part of melittin have a predominantly hydrophobic character, whereas the six amino acids at the C-terminus are very hydrophilic and basic. Melittin is soluble in both water and methanol. In water it is either monomer or tetramer and is shaped as a bent rod around residue Pro-14.^{31,32} In methanol melittin is a helical monomer with a bend angle of about 20°, significantly smaller than the 60° angle observed in water.³³ Various experimental studies have shown that melittin is helical in a lipid environment. The situation concerning the orientation of melittin in a phospholipid bilayer appears to be complex and sensitive to experimental conditions.^{30,34} Several experiments have indicated that in the peptide is oriented roughly perpendicular to the membrane surface,^{31,35} however there are also experiments (in the fluid phase of the bilayer) suggesting a parallel orientation.³⁰ The fact that a specific cationic C-terminus, which anchors the molecule in the vertical orientation, is required for lytic activity,^{36,37} as well as the fact that shortening the N-terminal sequences results in very poor lytic agents,³⁸ are two indications that the vertical orientation is indeed involved in lysis. When the peptide is membrane bound, residue Trp-19 is located approximately at the height of the C₁ atoms of the lipid hydrocarbon chains,³¹ leaving the six C-terminal amino acids outside of the hydrophobic region. This allows the C-terminus to interact with the polar head groups and the surrounding water. The ambiguity regarding peptide orientation, pertains also to computational studies which used simplified models to represent the melittin-membrane system. In one study the preferred orientation of the helix was found to be roughly perpendicular to the bilayer surface,³⁴ whereas another study indicated that melittin can adopt a wide range of orientations, from perpendicular to almost parallel.³⁹

On the basis of these and other observations,³⁰ three mechanisms for the lytic activity of melittin have been proposed. (1) Lysis is due to melittin-induced formation of ion-permeable water pores.⁴⁰ (2) Lysis results from the perturba-

tion of the lipid bilayer due to the presence of the peptide in the head group region.⁴¹ (3) Lysis occurs as a result of melittin aggregation.⁴² It seems that the first two mechanisms are best supported by the experimental data, although the third mechanism also has experimental support. In particular, experiments have shown that water molecules penetrate the hydrocarbon core of membranes more readily in the presence of membrane-bound proteins⁴³ or small peptides.⁴⁴ Specifically, it was found that melittin induces the formation of ion-permeable pores prior to lysis.⁴⁰ These findings are supported by MD simulations⁴⁵ showing that the rate of water translocation through the bilayer is limited by the interfacial region near the glycerol, which can be overcome by the presence of defects and vacuum at the interface. A membrane-embedded peptide clearly causes such defects.

Regardless of the lysis mechanisms assumed, whether the pore formation mechanism or the bilayer deformation mechanism, the molecular details of this process are yet unclear. In particular, it is unclear how lysis is related to the change in melittin's orientation, from being surface bound to being vertically embedded in the membrane, or in what way is water penetration induced. Several researchers suggested that partial translocation of melittin, which is initially bound parallel to the membrane surface, into the hydrophobic core is involved.^{25,46,47} Based on neutron scattering measurements at different bulk pH Bradshaw *et al.*⁴⁷ proposed that melittin with an unprotonated N-terminus binds parallel to the membrane surface, whereas melittin with a protonated N-terminus binds in a transbilayer way. Interconversion between the two binding modes appears to be possible under equilibrium conditions. Based on this proposal, as well as on their own MD simulations, Berneche *et al.*²⁵ suggested the following mechanism for membrane lysis. Melittin would initially bind parallel to the membrane surface with unprotonated N-terminus. Water molecules, and a rare hydrated hydronium ion, which transiently penetrate into the membrane interior can at some point protonate the N-terminus of the melittin, leading to a conversion into a transbilayer orientation.

A molecular level characterization of the association of melittin with membranes and its influence on the surrounding lipid and water phases, is necessary for a better understanding of the microscopic mechanism involved in the lytic event. Recently, two complementary MD simulations of melittin in a bilayer environment were reported.^{25,27} In the simulation of Berneche *et al.*²⁵ melittin was bound on a DMPC membrane surface in a parallel orientation, with its unprotonated N terminus slightly embedded in the hydrophobic core (a total of 10 000 atoms were included in the simulation). This simulation showed that protonation of the N-terminus (at the same orientation) induces significant penetration of water molecules into the bilayer. In a separate study, Bachar and Becker²⁷ simulated a melittin peptide (protonated N-terminus) embedded in a large DPPC bilayer in the transbilayer orientation (a total of 19 000 atoms were simulated, and the system consisted of a 70 DPPC phospholipid bilayer and more than 3000 water molecules). The results reported for that simulation focused on membrane/protein interactions, showing that the embedded peptide

perturbs the structure of the lipid bilayer, mainly of the lower (intracellular) layer, which hosts the peptide's N-terminus. Other structural effects, such as the correlated tilting of peptide and phospholipids, were also reported.

The present study focuses on the interaction between the membrane-embedded peptide and the surrounding water, and is based on the MD simulation of the hydrated DPPC/melittin system.²⁷ The peptide's effect on the water at the lipid/water interface is studied, and water penetration into the bilayer is characterized. The results are compared to experimental observations and discussed in the context of melittin's lytic activity, which is related to an increase in membrane permeability to water and other small molecules.

II. METHODS

The computational model and procedure were reported at length in Ref. 27. Here we give a shorter, though quite complete, description of the simulation.

A. Pure DPPC bilayer

The decision to use 1,2-dipalmitoyl-3-sn-phosphatidylcholine (DPPC) as the bilayer composing phospholipid was based on the fact that melittin's lytic effect is most significant in zwitterionic bilayers⁴⁸ and decreases with the length of the acyl chain.⁴⁹ DPPC is a zwitterionic phospholipid of a medium size chain consisting of 16 carbons. Namely, DPPC is short enough so that the effects of melittin can be studied, and yet it is long enough to be relevant for realistic biological membranes, which typically include 16 to 20 or 22 carbon long phospholipids. In addition, DPPC is one of the best-studied phospholipids, both by experiment and simulation.¹

The DPPC phospholipid bilayer model used in this study is based on the model developed by Feller and Pastor.¹³ MD simulations of this system under constant normal pressure, fixed surface area, and periodic boundary conditions were shown to be reliable and in agreement with experimental results.^{13,50} Feller and Pastor's results also support the validity of the empirical phospholipid force field included in the CHARMM 22b4 parameter set.^{51,52} The pure membrane model includes 72 DPPC phospholipid molecules arranged in a square 36×2 bilayer (with periodic boundary conditions) corresponding to the biologically active $L\alpha$ phase of the membrane. The bilayer is flanked by a 30 Å layer of TIP3P water (2509 water molecules, periodic boundary conditions in the direction normal to the bilayer). The size of the system $47.6 \text{ Å} \times 47.6 \text{ Å} \times 68 \text{ Å}$ was set to allow a 62.9 Å^2 area per phospholipid headgroup.^{13,53} The initial conformation of the pure bilayer model was received equilibrated from Feller and Pastor.¹³ An additional 100 ps of dynamics were performed on the pure membrane model, in order to obtain a baseline to which the melittin/bilayer system will be compared. Before embedding the peptide in the membrane, the water layer was broadened to about 40 Å to ensure full solvation of the peptide's C-terminus.²⁷ At the end of this preparatory stage the system included 3207 water molecules, and the dimensions of the simulation box were $47.6 \text{ Å} \times 47.6 \text{ Å} \times 80 \text{ Å}$.

The CHARMM molecular dynamics program⁵⁴ and the CHARMM all atom phospholipid forcefield⁵¹ were used. The SHAKE algorithm was applied to all bonds involving hydrogen atoms and a 2 fs time step was used. The non-bonded Lennard-Jones interactions were switched to zero over the region 12–14 Å. Ewald summation was used for the calculation of electrostatics.⁵⁵ Three dimensional periodic boundary conditions were applied and the cell length normal to the membrane was allowed to adjust to maintain a constant normal pressure of 1 atm, using a Langevin piston algorithm.⁵⁶ The simulation temperature, which was controlled by a Nose-Hoover thermostat, was 320 K, i.e., above the gel-liquid phase transition temperature for DPPC (314.5 K in multilamellar vesicles).⁵⁷ This temperature ensures that the system is at the biologically relevant fully hydrated liquid crystalline $L\alpha$ phase of the bilayer, yet it is low enough to ensure the stability of the embedded peptide.

B. Combined melittin/bilayer system

The large-scale motion involved in reorienting melittin, from the parallel orientation on the surface to the transbilayer orientation, is beyond the scope of MD simulations. Since this major conformation transition is too slow to be studied by MD, the orientation of the peptide relative to the membrane plane has to be predetermined when the simulation is being set up. In the present study, we chose to simulate melittin in its transbilayer orientation, perpendicular to the membrane surface. Following neutron scattering measurements of Bradshaw *et al.*⁴⁷ which suggest that melittin with unprotonated N-terminus binds parallel to the membrane surface, whereas melittin with protonated N-terminus binds in a transbilayer way, the N-terminus of melittin in the present study was protonated. The initial melittin coordinates, taken from the x-ray structure of Terwilliger and Eisenberg²⁹ (protein data bank entry 2 mlt), were minimized prior to membrane insertion (using the CHARMM molecular mechanics program⁵⁴ and force field⁵²).

The peptide was placed vertically into a cavity formed by removing two DPPC phospholipids from the center of the upper layer. The molecule was then rotated around its z axis to find the optimal rotational orientation that would best fit the cavity. The vertical alignment with the surface was according to the experimental observations³¹ that when the peptide is perpendicular to the bilayer plane its residue Trp-19 is slightly above the plane defined by the C_1 carbons of the lipid chains. Thirty-six water molecules were removed from the model due to overlaps with the peptide C-terminus amino acids. 200 steepest descent minimization steps of the peptide alone, followed by 2000 steepest descent steps of the combined model (peptide, phospholipids, and water) were required to relax the system and remove practically all bad contacts. At the end of this process the peptide was positioned nicely in the membrane. No significant cavities were formed due to the insertion process (as indicated from the fractional free volume²⁷). Although the embedded peptide also interacts with the lower layer of phospholipids, this layer was not specially treated because the peptide penetrates only the low-density region of this layer, near the membrane mid plane (see the density profiles in Fig. 2). The method

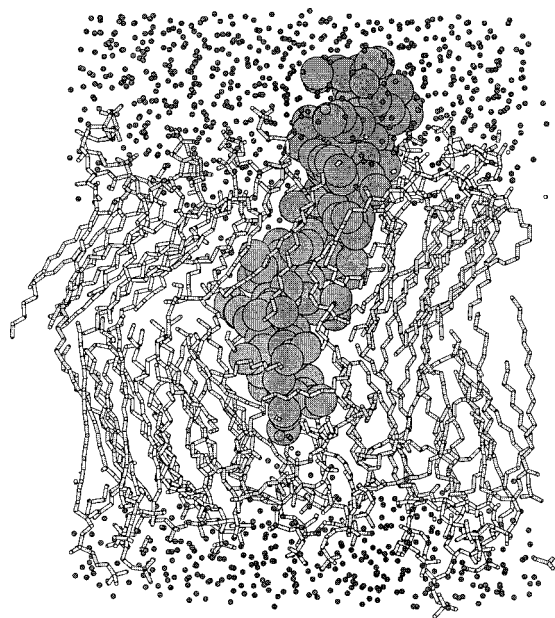


FIG. 1. A detailed view of the combined melittin/membrane/water system after 500 ps of molecular dynamics. The peptide is represented by space filling spheres. To obtain a clearer view, about half of the membrane phospholipids "in front" of the peptide as well as the hydrogen atoms of the acyl chains are not shown. The overall tilt of the peptide and of the phospholipids in the upper layer is clearly seen.

used in this study to place the peptide in the membrane resembles the method of Shen *et al.*²⁴ which was later adopted by Tieleman and Berendsen.^{26,28} In both methods the peptide is inserted into a precreated cavity in the membrane (although in the present study there was no need for an additional cylindrical repulsive force to expand the cavity). In the studies of Roux, Woolf, and collaborators phospholipids were added around a pre-existing helix.^{21–23,58}

The final combined model included the melittin peptide, 70 phospholipids, and 3171 water molecules. This system of 19 049 atoms was heated from 100 to 320 K over a 15 ps period and then simulated for 500 ps. Conformation snapshots were taken every 0.5 ps. All simulations were performed on an IBM SP2 supercomputer, at an average rate of 70 min/ps using 16–32 processors in parallel.

III. RESULTS

A. Structural characteristics melittin/bilayer system

Figure 1 depicts a snapshot of the membrane/peptide system after 500 ps of MD simulation (about half of the membrane phospholipids "in front" of the peptide were removed to ensure a clearer view).

The density profiles for key chemical groups in the bilayer system (phosphate, CH₂, CH₃, and water), averaged over the last 300 ps of the dynamic simulation, are shown in Fig. 2. This plots shows the density of chemical groups (groups per unit volume, unlike the standard atom per unit volume plots) highlighting the location of the membrane interface (the phosphate group) and the membrane's midsection (CH₃ groups). The atomic density of the embedded peptide is also shown. Overall the densities depicted in Fig. 2 are similar to those observed in a pure membrane. In particular

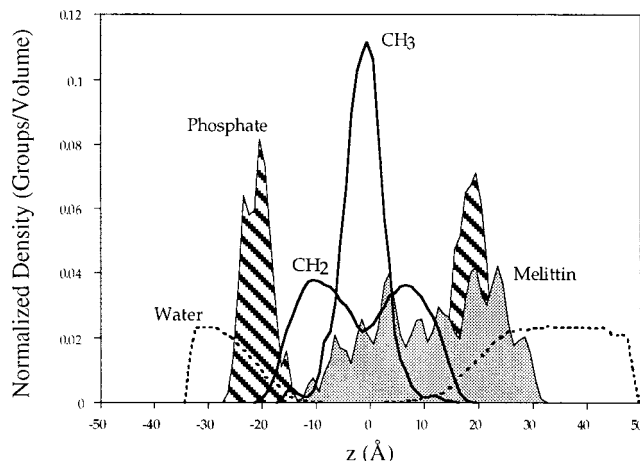


FIG. 2. The density profile of all key chemical groups in the combined membrane-peptide-water system (P atoms, CH₂, CH₃, water, and the peptide) averaged over the last 300 ps of the dynamics simulation. These density profiles are similar to those calculated for a pure membrane. Note the broad membrane interface (12 Å as reflected by the density of the phosphorous atom) and a very broad CH₃ peak (~14 Å on both sides of the membrane mid-plane). Normalized densities are calculated as chemical groups per unit volume, except for the melittin where density is calculated as atoms per unit volume.

the width of the interface (as reflected by the width of the phosphorous density peak) is 12 Å, similar to the values calculated for pure bilayers (10–13 Å).¹ Figure 2 also shows that the cationic C-terminus of the peptide (which includes four positively charged groups: Lys-21, Arg-22, Lys-23, and Arg-24) extend about 12 Å above the average membrane surface (defined by the phosphorous atoms) and is well solvated. The N-terminus of the peptide, on the other hand, penetrates approximately 10 Å into the lower half of the bilayer.

The structural properties of the membrane/peptide system, as well as the interaction between the lipids and the peptide, were discussed at length in the previous paper.²⁷ Some findings of importance to the present analysis are as follows. The DPPC embedded melittin does not remain perpendicular to the surface. Rather, the upper helical segment of the peptide adopts a 25° tilt relative to the membrane normal. The tilted conformation is clearly seen in Fig. 1. The peptide's tilt is coupled to a similar tilt of the phospholipids comprising the upper layer of the membrane. In addition, melittin adopts a 30° bend at residues Thr-10 and Pro-14 (between the two helical segments of the molecule). This bend is similar to the 20° angle observed in methanol, and significantly smaller than the 60° bend observed in water. Relevant to the present study is the unwinding of the peptide's N-terminal helix, which was observed in the simulation. This unwinding is strongest for residues Gly-1 to Gly-3, but affects residue Val-5 as well.

B. Water orientation normal to the membrane plane

The orientational polarization at different distances from the membrane is the most direct way to characterize interfacial water. Molecular dynamics simulations of pure membranes have shown taut water molecules at the phospholipid/

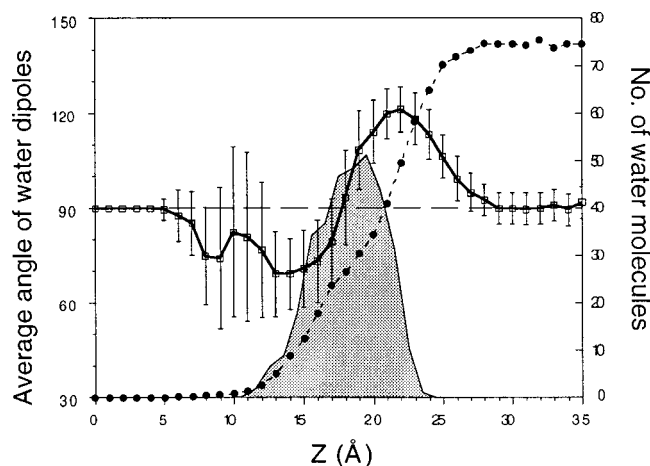


FIG. 3. The average orientation of water dipoles relative to the normal to the plane of a pure DPPC bilayer, as a function of distance along the normal direction (average over 100 ps of MD simulation). Also shown are the number of water molecules in each 1 Å slab as a function of normal distance (dashed line) and the density distribution of the phosphate atoms (shaded area, adapted from Fig. 2).

water interface exhibit a preferential order.^{3,16,17} Near the headgroups, within the lipid/water interface, the water molecules are oriented so that the positive ends of their dipoles point on average towards the bilayer interior. This orientation counters the normal components of the headgroup dipoles in membranes such as DPPC¹⁶ or DLPE.¹⁸ Far from the lipid/water interface water molecules are randomly oriented with respect to the plane of the membrane.

The orientation of interfacial water is measured by the average angle formed between the water dipoles and the normal to the membrane surface. Water molecules were grouped into 1 Å slabs parallel to the x - y plane, and the average angle of water dipoles in each slab with respect to the membrane normal was calculated. An angle of 0° reflects a water molecule whose dipole is pointing away from the phospholipid layer (i.e., its oxygen atom is pointing towards the membrane). An angle of 90° indicates a random orientational distribution of the water dipoles.

Figure 3 shows the average orientation of water dipoles in a pure DPPC bilayer in the direction normal to the membrane plane (average over 100 ps of MD simulation). Also shown are the number of water molecules in each 1 Å slab and the density distribution of the phosphate atoms (shaded area, adapted from Fig. 2). The orientational distribution depicted in Fig. 3 agrees well with previous observations.^{3,16,18} Over the 13 Å of the interface the water content increases from practically zero to its bulk value. In this interface region water dipoles adopt angles of up to 120° with respect to the membrane normal, indicating that on the average these dipoles point towards the bilayer. This value is similar to the 110°–115° angles reported in previous MD simulation of pure DPPC.^{16,17} It is interesting to note that water molecules at the membrane side of the interface adopt the opposite orientation, i.e., their dipoles point away from the membrane core. This trend is clear despite the large error bars (due to the small number of molecules).

An interesting question is: to what extent does the

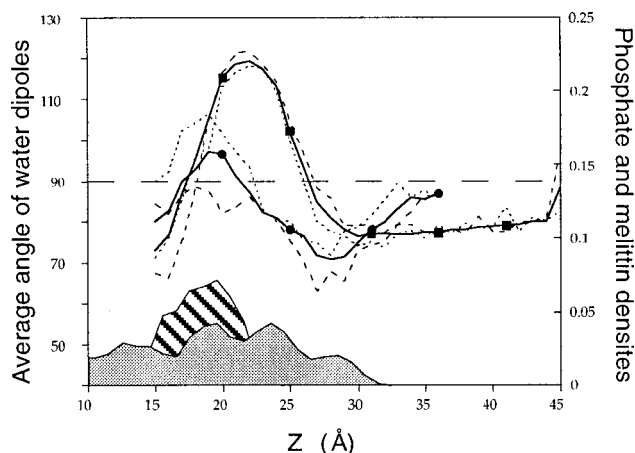


FIG. 4. The average orientation of water dipoles relative to the normal to the plane of the upper membrane layer in the combined melittin/DPPC system. To account for proximity to the peptide, the water molecules are divided into molecules which are close (within 12 Å) to the membrane-embedded peptide (circles) and those that far from it (squares). The solid lines depict an average over 500 ps of MD simulation. The orientational distribution averaged over the first 100 ps of the simulation (dashed line) and last 100 ps of the simulation (dotted line) are also shown. The density distributions of the phosphate atoms (dashed area) and of melittin (shaded area) are shown in order to give a reference frame (adapted from Fig. 2).

membrane-embedded peptide affect the orientational preferences of interfacial water? Figure 4 depicts the orientation of water dipoles (in the normal direction) on the extracellular side of the combined melittin/DPPC system. To highlight the effect of the peptide a distinction is made between water molecules that are close to the peptide (within 12 Å from any peptide atom) and water molecules far from it. Figure 4 shows the orientational distributions averaged over the whole 500 ps of the simulation, as well as averages over the first and last 100 ps of simulation. A striking difference between the orientation of water molecules close to the peptide and those far from it is observed. These results indicate that the peptide induces orientational disorder in its immediate vicinity destroying the orientational preference, which characterizes the pure membrane/water interface (Fig. 3). This orientational preference is restored for those interfacial water molecules that are far from the peptide (more than 12 Å away), which exhibit an average angle of up to 120° between their dipoles and the membrane normal.

A second effect, which has no parallel in pure membrane/water systems, occurs above the interface region (Fig. 4). In the presence of melittin water molecules above the interface also adopt a preferential orientation (unlike the random orientation that characterizes them in the absence of a peptide). Figure 4 shows that at $z \sim 27$ Å (lower for the “close” water), above the interface region, the water molecules reverse their orientation so that now their dipole moments point, on the average, not to but rather away from the membrane (an average angle of 70°–75°). This unique “reverse” orientation, which persists over a 15 Å range, occurs within the first 100 ps of the simulations and does not change afterwards. In general, temporal evolution is seen only for water dipoles close to the peptide, where the preferential orientation is partially regained with time.

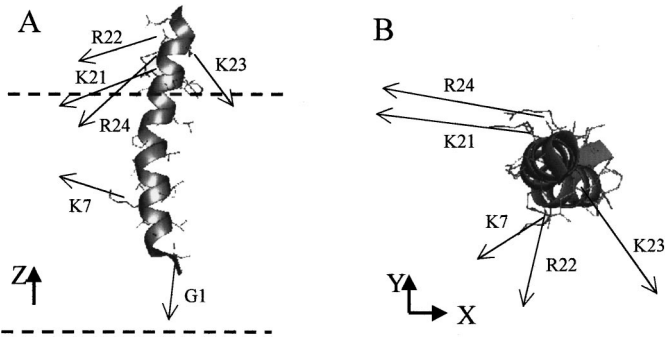


FIG. 5. The orientation and relative magnitude of six largest dipole moments of melittin, side view (A) and top view from the extracellular side (B). The six dipoles correspond to the four positively charged C-terminus residues Lys-21, Arg-22, Lys-23, and Arg-24, to the membrane embedded charged Lys-7 residue and to the positively charged protonated N-terminus. The average magnitude and orientation of these dipoles are summarized in Table I.

The above orientational effects are easily explained by the specific dipole moments of melittin. Figure 5 shows the orientation and relative magnitude of the six largest dipole moments of melittin. These dipoles are associated with the four positively charged C-terminal residues: Lys-21, Arg-22, Lys-23, and Arg-24, as well the membrane embedded charged Lys-7 residue and the positively charged protonated N-terminal Gly-1 (Table I). Only the four C-terminal dipoles are required to explain water orientation at the extracellular interface. As discussed above, water molecules orient themselves in response to strong dipole moments in their surroundings. The introduction of melittin changes this dipole environment affecting water orientation. Interfacial water molecules close to the peptide feel not only the normal component of the headgroup dipoles (which point away from the membrane), but also the strong normal dipole components of the C-terminal residues (which are directed towards the membrane). These two dipolar fields effectively cancel out (the normal contribution of the P–N dipoles is 3–9.5 D,⁵⁹ and that of the peptide residues is –5 to –15 D, see Table I). This cancellation leaves the water molecules without an external field to align against, hence the observed random orientation at the membrane/water interface near the peptide. Naturally, this cancellation effect is local to the immediate

TABLE I. The dipole moments melittin’s charged residues. Average dipole moment magnitudes, the normal components of these dipoles, and their orientation relative to the membrane normal are specified.

Residue	Dipole moment (D)	Normal component of dipole (D)	Dipole orientation (deg)
Gly-1	8.7±1.1	–8.3±1.0	–17.9±7.5
Lys-7 ^a	13.8±0.9	+5.1±0.3	+68.4±4.0
Lys-21	20.8±1.6	–11.9±0.9	–55.1±11.4
Arg-22	24.1±1.0	–16.2±0.7	–47.9±5.8
Lys-23	18.9±1.9	–5.2±0.5	–73.9±10.1
Arg-24	21.2±2.1	–10.9±1.0	–59.0±17.3
Other residues ^b	2–4		all negative

^aAverage over last 400 ps of the simulation. The average dipole moment during the first 100 ps is 8.5±0.5 D (see Fig. 5).
^bResidues Ser-18 and Gln-25 have dipole moments in the range 4–6 D.

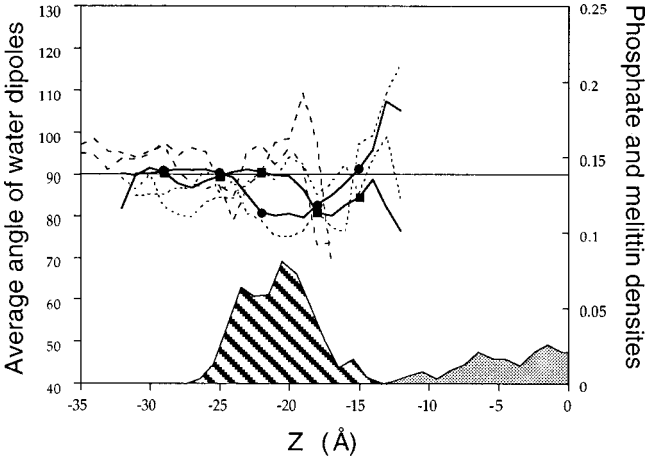


FIG. 6. The average orientation of water dipoles relative to the normal to the plane of the lower membrane layer in the combined melittin/DPPC system. Notation similar to Fig. 4. Close water molecules are defined within a 15 Å square column above the center of the lower membrane layer.

vicinity of the peptide. Away from the peptide, but still within the membrane/water interface region, water molecules regain their preferential orientation in response to the head-group dipoles. Water molecules above the interface, on the other hand, both near and far from the peptide, have only the peptide dipoles to align against. Since these dipoles are oriented towards the membrane plane, the bulk water molecules that feel this influence orient to counter them; i.e., with their dipole moments pointing away from the membrane.

Figure 6 shows the average orientation, in the normal direction, of water dipoles at the intercellular side of the combined melittin/DPPC system. As before, water molecules are grouped according to their distance from the peptide, even though the peptide does not reach all the way to the intercellular surface of the membrane. “Close” water molecules were defined as being within a 15 Å square column above the center of the lower membrane layer. The results depicted in Fig. 6 show a complete loss of dipolar orientation in the normal direction, both near to and far from the peptide. The average angle between the water dipoles and the bilayer normal is fluctuating around 90°. No clear time evolution is seen either. Because, water behavior at the lower interface cannot be explained by the melittin dipoles, the observed orientational disorder probably reflects a large-scale disorder in the structure of the lower membrane layer, which occurs in response to the peptide. This disorder, which will be discussed below, involves a significant amount of water penetration from the intracellular side as well as dislocation of several phospholipids in the lower layer.

C. Water orientation parallel to the membrane plane

The presence of the peptide is expected to affect the orientation of water dipoles not only in the normal direction, but also parallel to the membrane plane. To account for the spherical symmetry around the peptide the x-y plane was divided into four quadrants. The average angle between the water dipoles and the diagonal in each quadrant, pointing away from the center, was calculated (Fig. 7). As before, a

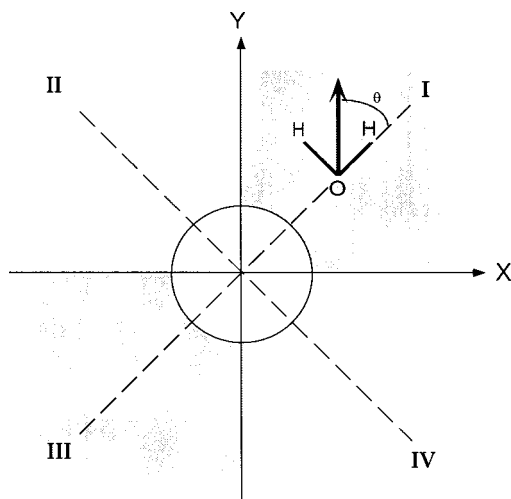


FIG. 7. A schematic illustration of how water-dipole orientations in the x - y plane, parallel to the membrane surface, were calculated. The plane was divided into four quadrants, and the average of the angle θ between water dipoles in each quarter and the diagonal pointing away from the peptide is calculated. A $\theta=90^\circ$ value indicates a random orientation, while $\theta=0^\circ$ reflects a preferential orientation with the dipoles pointing away from the peptide; i.e., the oxygen atoms pointing towards the peptide.

random distribution results in an average angle of 90° , a preferential orientation in which the oxygen points towards the peptide is indicated by an angle smaller than 90° , and the reverse by an angle larger than 90° . The distinction between water molecules close and far from the peptide was retained.

Figure 8 depicts the average orientation of water dipoles in the x - y plane parallel to the extracellular bilayer surface. The average orientations of water dipoles in each quadrant, for both close and far water molecules, are shown as a function of time (averages over the five 100 ps time intervals). Also shown are averages over the four quadrants and over the entire length of the simulation. For comparison, Fig. 8 also includes the orientation of water molecules parallel to the membrane plane in a pure DPPC/water system (averaged over 50 ps of dynamics). As expected, the "parallel" orientation of the water dipoles in the pure membrane/water system was random (average angles close to 90°).

Figure 8 clearly indicates that water dipoles close to the peptide exhibit a preferential orientation in the plane parallel to the membrane. The average angle for these molecules, averaged over all four quadrants and the entire simulation, was found to be 43° varying in a $\pm 30^\circ$ range. Namely, these water molecules are oriented with their negative oxygen atoms pointing toward the positive C-terminal segment of the peptide. This effect is limited to the immediate vicinity of the peptide. Water molecules away from the peptide were, on the average, not effected by the peptide (an average angle of 89° varying in a $\pm 48^\circ$ range).

Specific dipole orientations of the "close" water molecules vary significantly from one quadrant to the other (Fig. 8). The smallest angle between the water dipoles and the quadrant diagonal in the plane parallel to the bilayer surface, $37^\circ \pm 29^\circ$, was found in the second quadrant, indicating that molecules in this quadrant are those most effected by the peptide. Similar, though slightly larger values of $39^\circ \pm 33^\circ$

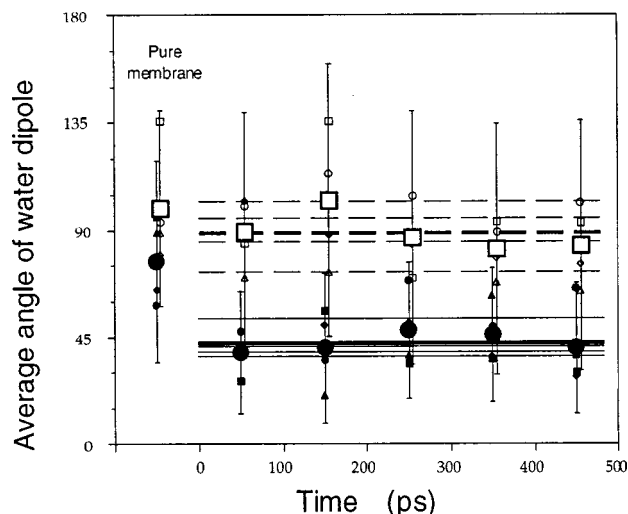


FIG. 8. The average orientation of water dipoles in the x - y plane parallel to the bilayer surface, for water molecules on the extracellular side of the membrane. The orientation is measured as the average angle between the water dipoles in each of the four quadrants (small symbols) and the diagonal pointing away from the embedded peptide (see Fig. 7). The quadrants are marked as follows: (circle) first quadrant, (square) second quadrant, (triangle) third quadrant, (diamond) fourth quadrant. The large symbols indicate averages over the four quadrants. Water molecules close to the peptide are designated by filled symbols; water molecules far from the peptide are marked by open symbols. The average orientations are shown as a function of time. Individual symbols indicate averages over 100 ps time intervals, while the horizontal lines indicate the averages over the entire 500 ps of the simulations (thin lines indicate individual quadrants, heavy lines are averages over all four quadrants; dashed lines are for water molecules far from the peptide). For comparison, the equivalent orientation of water molecules in a pure DPPC/water system is also shown (averaged over 50 ps of dynamics). Random dipole orientations are seen for water molecules far from the peptide and for water in the pure membrane/water system. Water molecules close to the peptide are oriented with their negative oxygen atoms pointing towards the positive peptide C-terminal segment.

and $41^\circ \pm 23^\circ$ were calculated from the fourth and third quadrants, respectively. Water dipoles in the first quadrant were less oriented exhibiting an average value of $53^\circ \pm 37^\circ$. These orientational preferences correlate very nicely with the peptide's C-terminal dipoles, which lay preferentially in the second and fourth quadrants, with a significant contribution in the third quadrants as well [Fig. 5(b)]. The first quadrant, on the other hand, is devoid of any large peptide dipole. No significant temporal evolution is observed in the data shown in Fig. 8, indicating that water orientation in the x - y plane occurs on a scale shorter than 100 ps.

Figure 9 shows the average "parallel" orientation of water dipoles at the intracellular bilayer interface. Unlike the marked effect seen for the water dipoles close to the peptide in the extracellular side, the effect on the intracellular side is much smaller. The average angle between the water dipoles and the quadrant diagonal in the parallel plane was $65^\circ \pm 50^\circ$ for water molecules close to the center of the lower layer (averaged over all quadrants and all times). Namely, these water molecules are oriented in the x - y plane with their dipoles pointing away from the center. This order is surprising in view of the fact that the same water dipoles have no preferential orientation in the direction normal to the membrane plane (Fig. 6). It is likely that the main contribution to this orientation is from water molecules that have penetrated

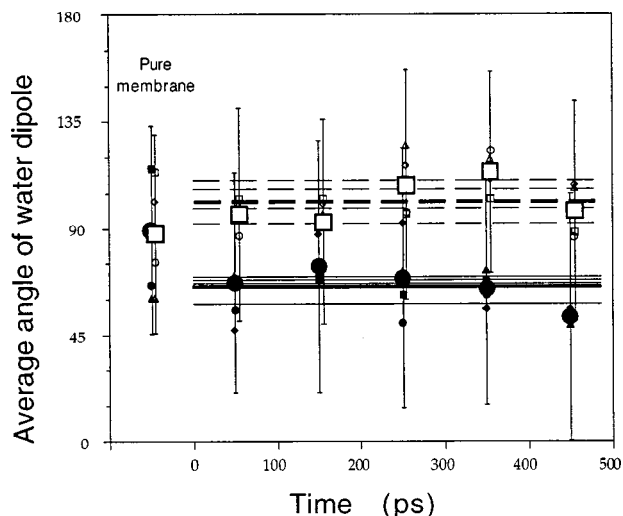


FIG. 9. The average orientation of water dipoles in the x - y plane parallel to the bilayer surface, for water molecules on the intracellular side of the membrane. Notation as in Fig. 8.

into the membrane. As will be discussed below, in the presence of the peptide, a significant number of water molecules penetrate from the intracellular side of the bilayer. These molecules orient their dipoles away from the peptide's protonated N-terminus, thus affecting the overall statistics. Support for this hypothesis comes from the high level of orientational fluctuations exhibited by these dipoles, reflecting a wide variation in water orientations ($\pm 50^\circ$ fluctuations compared to the smaller $\pm 30^\circ$ fluctuations on the extracellular side). The average angle for water molecules far from the center of the lower layer was $102^\circ \pm 48^\circ$, statistically equivalent to the 90° angle of a random orientation.

D. Penetration of water into membrane

Melittin-induced penetration of water molecules into the hydrophobic core of the membrane, which leads to the formation of water pores, is assumed to be a key process by which melittin disrupts the cell's membrane causing lysis. The present MD simulation verifies this process, as a significant amount of water penetration into the bilayer is seen. Moreover, the detailed information obtained from the MD simulation allow us to shed light on the microscopic mechanism involved, and on the molecular factors that drive the pore formation process. Overall, we find that this specific peptide induces water penetration from *both sides* of the membrane. It should be noted, however, that these conclusions are restricted of the presumed *trans* bilayer orientation of the peptide. Large orientational transitions, such as those that can be undergone by the peptide, will definitely affect water penetration, probably increasing it.

Figure 10 presents two snapshots highlighting water penetration into the hydrophobic core of the membrane. The snapshots, which show water molecules in the immediate vicinity of the peptide, are taken at the beginning of the simulations (after the initial 10 ps heatup phase) and at the end of the simulation, after 500 ps of dynamics. The plotted water molecules are within 5 \AA from the peptide on the extracellular side and within 12 \AA of the peptide on the intra-

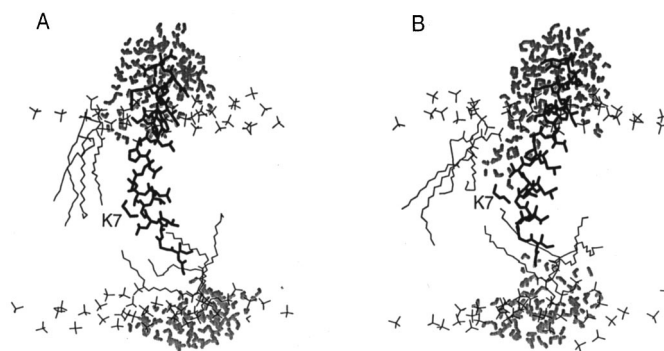


FIG. 10. Two snapshots highlighting the penetration of water molecules, in the immediate vicinity of the peptide, into the hydrophobic core from both sides of the membrane. One snapshot taken at the beginning of the simulations, only after the initial 10 ps heatup phase (A), and another taken at the end of the simulation after 500 ps of dynamics (B). Phosphate groups and a few lipids are also shown. Water penetration occurs from both sides of the membrane. On the extracellular side water penetrates up to residue Lys-7 (marked in the plot as K7). On the intracellular side water penetrates up to the protonated N-terminus of the peptide.

cellular side. The peptide, the phosphate groups, and a few lipid chains are also shown. As is clearly seen, water penetration occurs from both sides of the membrane. On the extracellular side water penetrates up to residue Lys-7 (marked in the plot as K7), and on the intracellular side water penetrates up to the protonated N-terminus of the peptide. Although a complete *trans*membrane water pore was not formed during the 500 ps of the dynamics, we find that by the end of the simulation water traverses about 3/4 of the membrane's width. It can be argued that it is only a matter of time before the two water bodies connect.

Figure 11 shows the number of water molecules penetrating the hydrophobic core of the bilayer from both sides. The amount of water penetrating into the bilayer from the extracellular side is evaluated by counting water molecules within 7 \AA from the peptide, in a volume extending between residues Ile-17 and Lys-7. The choice of residue Ile-17, just below the membrane/water interface, ensures that interfacial

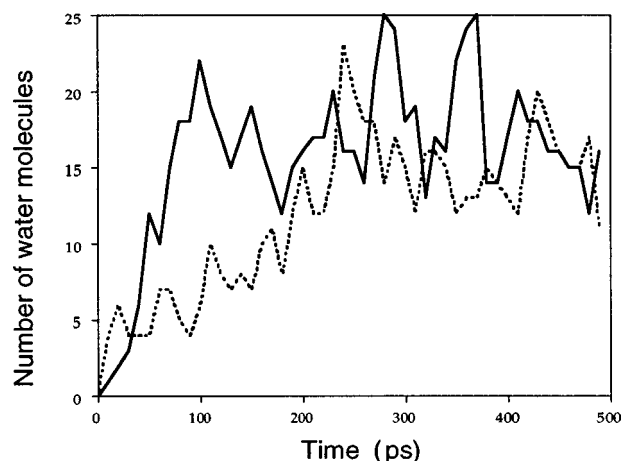


FIG. 11. The number of water molecules penetrating the membrane's hydrophobic core during the 500 ps of the MD simulation. The solid line reflects water molecules penetrating from the extracellular side; the dashed line reflects water molecules penetrating from the intracellular side (for the precise definitions see text).

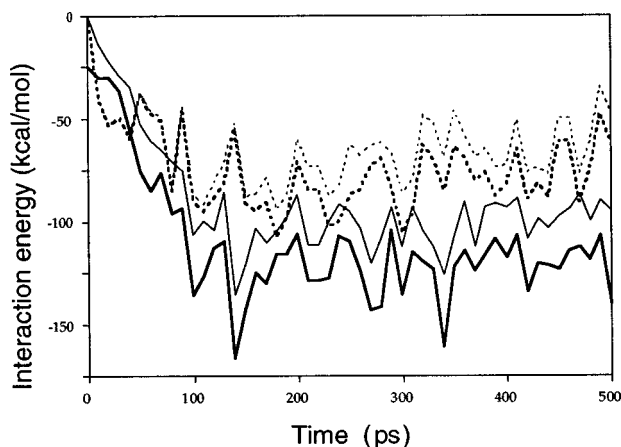


FIG. 12. The interaction energies between the membrane-penetrating water molecules and the peptide as a function of time. Shown are the interaction energies of the water molecules penetrating from the extracellular side to melittin residues 7–20 (heavy solid line) and to residue Lys-7 by itself (thin solid line). Also shown are the interactions of the water molecules penetrating from the intracellular side to the whole melittin molecule (heavy dashed line) and to the protonated N-terminus by itself (thin dashed line).

water molecules are excluded. On the intracellular side the enumeration was over water molecules within 11 Å from the peptide, in a volume extending from residue Ile-2 to the average plane of the lower layer's phosphate groups. Note that there is an inherent error in this enumeration, because the above volumes change slightly in the course of the simulation. To highlight water penetration during the simulation, the number of water molecules present in these volumes at time $t=0$ was subtracted from all subsequent values (12 water molecules in the upper volume, and 15 in the lower volume). Water molecules present at time $t=0$ were either transiently diffusing molecules, or interfacial water molecules, which slightly penetrate into the enumeration volume.

For both intracellular and extracellular penetration, the amount of water in the hydrophobic region rises gradually and then levels off. Water penetration from the upper layer increases over a 100 ps period and levels off at 18 ± 3 molecules. Water penetration from the intracellular side takes longer, about 200 ps, and levels off at 15 ± 3 molecules. No water molecules were found in the volume between Lys-7 and Ile-2 (close to the peptide). Thus, after about 200 ps of simulation the number of water molecules in the hydrophobic core of the membrane reaches 33 ± 6 , spanning approximately 3/4 of the membrane's width. These numbers compare well with the experimental results of Bradshaw *et al.*⁴⁷ which estimated the number of water molecules in the hydrophobic region of the membrane for each melittin as ~ 20 –30. Their observation that water penetration near the protonated N-terminus causes a loss of the α -helical structure for residues Gly-1 to Val-5 also agrees well with the behavior observed in the present simulation (see above).²⁷ A slightly smaller number of penetrating water molecules, approximately 15–25, was found in the simulation of Berneche *et al.*²⁵ in accord with the fact that melittin in that simulation was placed parallel on the extracellular membrane plane.

Figure 12 depicts the interaction between the peptide and the two penetrating water bodies (defined above). For water

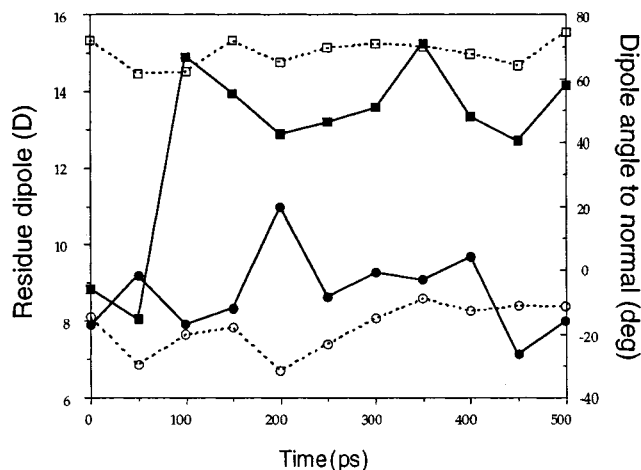


FIG. 13. The magnitude (solid line) and orientation relative to the bilayer normal (dashed line) of the dipole moments of melittin residue Lys-7 (squares) and the protonated N-terminus Gly-1 (circles) as a function of time.

molecules penetrating from the extracellular side Fig. 12 shows that their interaction with melittin residues Lys-7 to Ile-20 and with residue Lys-7 by itself follow a similar pattern. Starting from zero, the average interaction with Lys-7 reaches -100.4 ± 11.0 kcal/mol (5.6 kcal/mol per water molecule) while the average interaction with the whole membrane-embedded part of the peptide is only slightly stronger, averaging -121.9 ± 12.7 kcal/mol (about 6.8 kcal/mol per water molecule). This indicates that the largest contribution to the interaction between these water molecules and the peptide is from the charged residue Lys-7. A similar behavior is observed for water molecules penetrating from the intracellular side. Figure 12 shows that in this case the interaction is governed by a positively charged protonated N-terminus. Starting from zero, the average interaction of these molecules with the N-terminus reaches -62.6 ± 14.0 kcal/mol (about 4.2 kcal/mol per water molecule), while the interaction with the whole 26 residue peptide is -76.2 ± 14.4 kcal/mol (about 5.1 kcal/mol per water molecule).

These results, which indicate that penetrating water interacts primarily with the two membrane-embedded charges, Lys-7 and the protonated N-terminus, suggest that these two have a key role in steering water penetration. Indeed, Fig. 5 and Table I indicate that the dipole of Lys-7 is the only melittin dipole moment that points from the membrane interior towards the extracellular surface, and that the dipole of the protonated N-terminus points directly at the intracellular surface of the membrane. The role of these two dipoles as “beacons” is demonstrated in Fig. 10(b), which shows that water penetrating from the extracellular side move directly towards residue Lys-7, while water penetrating from the intracellular side move towards the peptide's N-terminus. Figure 13 depicts the magnitude and orientation (relative to the bilayer normal) of these two peptide dipoles. Figure 13 shows that the orientation of both dipole moments remains unchanged throughout the simulation (standard deviation of $\pm 4.0^\circ$ for Lys-7 and $\pm 7.5^\circ$ for the N-terminus), reflecting similarly restricted motions of the Lys-7 side chain and of

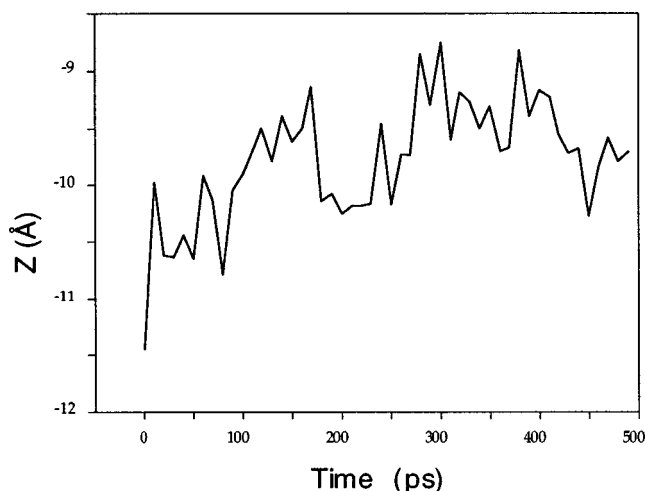


FIG. 14. The normal Z coordinate of the phosphate atom in one phospholipid (from the lower layer) that is being moved as a result of water penetration from the intracellular side. The headgroup of this phospholipid moves as much as 2 Å into the bilayer.

the N-terminus. It also shows that within the first 100 ps of the simulation the dipole moment of residue Lys-7 increases from an average value of 8.5 ± 0.5 D to an average value of 13.8 ± 0.9 D. Given the fact that the motion of the Lys-7 side chain is very restricted, the abrupt increase in dipole moment indicates that the lysine side chain has “stretched out,” resulting in a greater dipole moment. Comparing the variation in the Lys-7 dipole moment (Fig. 13) to the number of water molecules penetrating from the extracellular side (Fig. 11) reveals that the two phenomena are correlated. This correlation suggests that the change in Lys-7 dipole is due to its tendency towards solvation by the incoming water molecules.

Finally, while the phospholipids surrounding the penetrating water molecules on the extracellular side do not exhibit significant deformations, this is not the case in the lower layer of the membrane. A significant degree deformation of the lower lipid layer in the vicinity of the peptide N-terminus is seen. It seems that the penetrating water molecules push some phospholipids out of the way. Most striking is the response of one of the phospholipids closest to the N-terminus, which in response moves deeper into the bilayer. Figure 14 shows the position of the phosphate atom of this phospholipid as a function of time. Within the first 200 ps, in which water penetration into the intracellular side occurs, the headgroup of this phospholipid moves as much as 2 Å deeper into the bilayer. Smaller deformations were observed in a few other phospholipids in that vicinity. This deformation correlates well with the loss of water dipole orientation in the direction normal to the membrane plane, observed for water dipoles on the intracellular side of the bilayer (Fig. 6).

IV. DISCUSSION

Proteins are an important component of biological membranes. One of the ways in which proteins affect membrane processes is by changing the behavior of water molecules at the membrane interface, and by inducing water penetration

into the bilayer. Thus, membrane-bound proteins can induce the formation of ion channels, enhance permeation of water through the membrane, and cause membrane lysis. Experimental techniques, despite their wealth of insightful information, can rarely probe the microscopic details of such processes. The MD simulation reported in this paper sheds light on the detailed microscopic events involved in the effect of a membrane-embedded peptide, in this case melittin, on the water molecules surrounding the combined membrane/peptide system. Two processes were the focus of the present analysis: (a) peptide-induced changes in the orientation of the water molecules at, and above, the membrane/water interface; and (b) peptide-induced penetration of water into the hydrophobic core of the bilayer. Recall, that in the present simulation the melittin peptide had a protonated N-terminus and was oriented perpendicular to the membrane plane (following recent experimental observation).⁴⁷

It should be noted that because melittin can undergo a large-scale orientational transition, from being surface bound to being membrane embedded in the transbilayer orientation, the present study can give only a partial insight into its overall effects. Clearly, any specific melittin orientation should be considered as transient on the scale of the full peptide insertion process (even if it is stable on the time scale accessible to present day molecular dynamics simulations). It is thus possible that features such as water pores, discussed in the present study are not stable on much longer time scales.

A. Orientation of water molecules at the membrane interface

The results of the simulation show that the membrane-embedded peptide affects the orientation of water dipoles at, and above, the membrane interface. Somewhat surprisingly we find that the peptide affects the orientation of water molecules on both sides of the membrane, not only on the extracellular side in which it is anchored. The effects at the intracellular side of the membrane occur despite, or perhaps because of, the fact that the peptide's N-terminus does not reach as far as the lower membrane surface. The microscopic characteristics, however, are different for water molecules on each side.

On the extracellular side the peptide has a disorienting as well as an orienting effect on water dipoles in its immediate vicinity. In the direction normal to the membrane melittin disrupts the typical preferential orientation of water dipoles at the membrane interface. The strong dipoles of the charged C-terminal residues, which point towards the membrane surface, counter the headgroup dipoles, leaving no external field for the water to orient their dipoles against. On the other hand, melittin's charged C-terminus induces a preferential orientation in water molecules above the interface region (instead of the random orientation in the absence of the peptide). A similar orientational preference, in response to the dipoles of melittin's charged C-terminus, is also observed in the plane parallel to the membrane surface. The MD simulations showed that water dipoles in the x - y plane were preferentially oriented with their dipoles pointing away from the peptide; i.e., with their negative charged oxygen atoms pointing towards the positive charged C-terminus.

The response of the water dipoles on the intracellular side of the membrane showed a similar complex pattern. In the direction normal to the plane of the membrane the peptide caused the destruction of any preferential orientation of the water dipoles. Water dipoles close to the center of the lower phospholipid layer had no preferential order, both at the interface region and outside towards the bulk. This behavior, which is in marked contrast to the preferential orientation in a pure bilayer system, is probably coupled to two other observations: water penetration from the intracellular side towards the protonated N-terminus and the disruption of the phospholipid surface itself. These indicate an overall disruption of the order of the lower membrane layer, which is reflected in the orientation of water dipoles in the intracellular interface. Evidence for this disrupted structure were reported in our previous paper.²⁷ This phenomenon is also attested by the dislocation of headgroups in the vicinity of the peptide's N-terminus. Despite the orientational disorder in the normal direction, water dipoles close to the center of the lower membrane layer exhibited order preferences in the plane parallel to the membrane surface. This effect is probably dominated by membrane penetrating water molecules that orient their oxygen atoms towards the peptide, in response to the positive charge at the N-terminus.

B. Formation of water pores

The MD simulation results indicate that transmembrane water pores are formed when melittin is added into a phospholipid bilayer. Although a fully connected transmembrane water pore was not formed during the 500 ps of the simulation, such a pore was clearly in the making. Within as little as 200 ps the positively charged melittin induces water penetration into the hydrophobic core from both extracellular and intracellular sides of the membrane. This "two sided" penetration pattern increases the likelihood of forming a transmembrane water pore. In response to the peptide's presence, water molecules transverse about 3/4 of the membrane's width within a very short time period. As a result, the distance between the two water bodies on both sides of the membrane abruptly reduces from approximately 40 Å to a mere 10 Å gap. The water molecules' diffusive motion can cover the remaining short distance quite easily, thus completing the formation of the pore. This process, however, is expected to be slower than the initial penetration, since additional energy barriers are to be crossed. The observed penetration pattern, from both sides of the membrane, indicates that the water pore that is being formed has a broad cross section, very different from a hypothetical single-file water pore. The formation of a relatively broad water pore is in good agreement with the experimental observation. While single-file pores may be efficient for proton transfer, as has been recently shown by Marrink *et al.*,⁶⁰ only relatively broad pores can account for the experimentally observed ion permeation prior to full lysis.⁴⁰

The melittin-induced formation of a broad water pore seen in the simulation is in good agreement with experiments. Tosteson *et al.*⁴⁰ suggested that hemoglobin release in melittin-induced lysis is secondary to the formation of ion-permeable pores. This conclusion was based on the observa-

tion that treatment with melittin prior to lysis induces the following effects: (1) A 200-fold increase in ion permeability over the first minute (before release of hemoglobin); (2) swelling of the cells before they break; and (3) replacing salts with high molecular weight osmolytes in the extracellular medium inhibits lysis. The ion permeability of melittin-induced pores was attested to by several studies, which showed that melittin induced water pores are selective for anions over cations.^{38,40,61} This means that the observed melittin-induced formation of ion-permeable channels in a manner of voltage-gated pores has much in common with melittin-induced lysis. Indeed, despite the evidence that lysis does not require voltage-dependent pore, Clague and Cherry⁶² showed that the lysis activity of melittin increases with the increase in the transmembrane potential.

The simulation results are also in good agreement with recent neutron scattering measurements, from which Bradshaw *et al.*⁴⁷ estimated the number of water molecules (or hydrated protons) in the hydrophobic region of the membrane as ~20–30 molecules for each melittin peptide. These experiments also indicate that the N-terminal segment Gly1 to Val5 loses its α -helical conformation as a result of water penetration near the protonated N-terminus. Both observations are reproduced in the present simulation. The number of water molecules penetrating the bilayer in the simulation was about 30 water molecules per peptide, and the N-terminal segment of melittin had indeed unwound itself during the 500 ps of the simulation. A similar amount of water penetration was observed in the MD simulation of Berneche *et al.*,²⁵ approximately 15–25 water molecules, in response to protonating the N-terminus (the peptide was roughly parallel to the extracellular surface).

The amount and pattern of water penetration into the hydrophobic core of the membrane, in response to the presence of melittin, is thus in agreement with a variety of experimental observations. The MD simulation, however, can also offer a unique insight into the microscopic mechanism involved in melittin-induced pore formation. The microscopic mechanism attested to by the simulation, which highlights the special role of residue Lys-7 and the protonated N-terminus, is discussed below.

C. Monomer versus tetramer

The MD simulation indicates that water penetration and pore formation does not require tetramerization of melittin in the membrane. Various researchers^{31,61} suggested that the formation of ion-permeable pores through the membrane occurs upon a tetrameric association of four melittin monomers. Our results, though not definitive, seem to indicate that tetramerization is not required for the formation of water pores, as they can be formed by a single melittin molecule. This conclusion, that tetramerization is not an essential requirement for lysis, is in agreement with experiments in which melittin analogs retained lytic activity even though they did not become tetrameric.⁶³ Neither results, however, preclude the possible formation of melittin tetramers not do they refute their role as an alternative route to lysis (possibly activated at high melittin concentrations).

D. Role of residue Lys-7

The microscopic mechanism, arising from the above simulation indicates that residue Lys-7 plays a key role in the formation of transmembrane water pores. In fact, this residue is the primary factor driving water penetration from the extracellular side of the membrane into the bilayer. Lys-7 is the only melittin residue, except for the protonated N-terminus, embedded in the bilayer's hydrophobic core that is positively charged. The large dipole associated with of this charged residue is also the only melittin dipole pointing 'upwards' towards the extracellular membrane surface (Fig. 5 and Table I). Therefore, the Lys-7 dipole acts as an electrostatic "beacon" attracting water molecules from the extracellular side of the membrane, steering their penetration halfway into the bilayer. The interaction between Lys-7 and the water molecules is primarily electrostatic in nature. It is thus not surprising that experimentally it was found that melittin induced ion-permeable pores exhibit selectivity for anions over cations,^{38,40,61} supporting the role of the positively charged Lys-7.

The role of Lys-7 in the formation of ion-permeable pores was hypothesized by several researchers,^{31,61,64} but it is only through MD simulations that direct evidence as well as a microscopic mechanism for its function can be offered. Experimental support of the important role of residue Lys-7 in inducing lysis was obtained by Blondelle and Houghten⁶⁴ in their study of melittin omission analogs. In that study the lytic activity of 24 single omission analogs of melittin was studied and compared to native melittin. Except for the dramatic effect of omitting hydrophobic residues, which reduces the overall hydrophobicity of the molecule, only two nonhydrophobic residues were identified as having an important role in lysis: Trp-19 and Lys-7. The 30-fold decrease in activity upon omission of Lys-7 indicates that the positive charge on Lys-7 has a specific role in the lytic activity of melittin. This conclusion is supported also by the loss of activity upon substituting Lys-7 for a leucine residue⁶⁵ and by the loss of activity brought about by succinylation of the ϵ -amino groups of lysine residues in melittin.³⁷ In this second experiment the loss in activity arises primarily from the absence of a positive charge in position 7 (the two other lysine residues are at the C-terminal positions 21 and 23). Nonetheless, there is a single experimental result, which contrasts the above observations, reporting that lytic activity was retained upon N-acetylation of all lysine residues and of the N-terminal group of melittin.³⁶ It is possible that in that case an alternative lysis mechanism, not involving the formation of water pores, was involved. Finally, another indication for the role of Lys-7 is found in the experiments of Weaver *et al.*⁴⁶ which showed that the N-terminal segment of melittin (which in their study included both Lys-7 and the N-terminus Gly-1) has a central role in the membrane lysis activity.

E. Role of N-terminus

While residue Lys-7 plays an important role by attracting water molecules from the extracellular side of the membrane, the MD simulation results indicate that the protonated

N-terminus plays an equally important role on the intracellular side. The positive charge and the N-terminal dipole, which is oriented directly at the intracellular membrane surface, induce water penetration from the intracellular side of the membrane into the lower phospholipid layer. The significant amount of water penetrating towards the protonated N-terminus is associated with a major deformation of the membrane surface near the peptide's N-terminus.

The important role of the protonated N-terminus is also supported by experimental observations. Extensive experiments by Weaver *et al.*⁴⁶ have shown that the N-terminal segment of melittin (which in their study included both Lys-7 and the N-terminus Gly-1) has a central role in the mechanism of membrane lysis. In a different experiment, Gevod and Birdi³⁸ found that the length of the N-terminal helical segment is important for cell lysis, as melittin analogs with shortened N-terminal sequences were very poor lytic agents. This observation was originally interpreted as indicating a destabilization of the peptide's binding to the cell membrane. Our simulation seems to suggest an alternative (or additional) explanation for the observed phenomenon. In the perpendicular peptide orientation, in which the peptide is anchored to the extracellular side through the C-terminal segment, shortening the N-terminus has the effect of moving the associated dipole away from the opposite membrane interface. As this dipole is being moved away from the intracellular interface its ability to induce water penetration from that side reduces, and so does the observed cell lysis.

F. Importance of melittin's bend and tilt

The aforementioned simulations also indicate that the melittin-induced formation of transmembrane water pores relies on the specific bent conformation of melittin. Our previous study²⁷ has shown that in a DPPC bilayer melittin adopts a 30° bend angle, between the C-terminal helix and the N-terminal helix, as well as a 25° tilt relative to the membrane normal (coupled to a similar tilt of the phospholipids in the upper layer). These conformational characteristics, which can be seen in Fig. 1 and Fig. 10(b), mean that while the upper half of the peptide is tilted by 30° relative to the membrane normal, the peptide's N-terminus is pointing directly at the lower membrane surface. This specific combination of bend and tilt angles has an important consequence as far as lysis is concerned. These conformational factors align the two functional dipoles, the protonated N-terminal dipole and the dipole of Lys-7, in the appropriate directions for inducing water penetration.

It was argued that the Lys-7 dipole, which forms a $+68^\circ \pm 4^\circ$ angle with the membrane normal, acts as the beacon attracting water molecules from the extracellular side of the membrane. If, for example, the C-terminal helix of the peptide was not tilted by 25°, this important Lys-7 dipole would have been oriented parallel to the membrane surface (forming a $\sim 90^\circ$ angle relative to the normal direction), rendering it completely inefficient for inducing water penetration into the bilayer. A similar argument is true for the N-terminal dipole. The orientation of this dipole directly at the intracellular membrane surface, forming an $18^\circ \pm 7^\circ$ angle with the membrane normal, allows it to open a conduit for water mol-

ecules to penetrate the membrane from the intracellular side. If, for the sake of argument, the peptide was not bent by 30° , the consequence would have been for the N-terminal dipole to form a $\sim 50^\circ$ angle with the normal direction. This would have significantly reduced the normal component of that dipole, from 8.3 ± 1.0 D to approximately 5.5 D, thus diminishing its ability to steer water penetration. Therefore, it is through this specific conformation and orientation that melittin can satisfy the otherwise contradictory orientations of these two functional dipoles.

The conclusion, that water pore formation relies on the bent structure of melittin, is supported by experiments in which the activity of a synthetic melittin analog, [Ala-14]melittin, was studied.⁴¹ Note that this analog, in which the helix-breaker residue Pro-14 was replaced by a helix-forming residue Ala-14, is expected to form a straight, non-bent helix. It was found that although [Ala-14]melittin increases lysis relative to native melittin, it has poor voltage-gated channel activity in planar bilayers. This means that the nonbent peptide is indeed a poor water pore former, and that its induced lysis probably occurs through a different mechanism, e.g., by perturbing the structure of the bilayer.

As the present simulation started from a preoriented melittin in the direction perpendicular to the membrane surface, it cannot address the very important issue of conversion from the surface-bound parallel orientation (studied recently by Berneche *et al.*²⁵) and the transmembrane orientation (studied in this work) of melittin. The change in orientation is beyond the scope of today's MD simulations.

G. Structural perturbation vs "pore" formation

As discussed above, several different mechanisms were proposed for melittin-induced membrane lysis. The two best supported mechanisms for this lytic process are melittin-induced formation of ion-permeable water pores⁴⁰ and perturbation of the lipid bilayer due to the peptide's presence.⁴¹ Both mechanisms result in the destruction of the cell's membrane, and both are compatible with many experimental observations. In the present paper, which focused on the behavior of water in the presence of the membrane-embedded peptide, it was shown that the MD simulation reflects the formation of melittin induced water pores, thus supporting the first mechanism.

This result, however, does not preclude a simultaneous role for the second mechanism, in which lysis is induced by a perturbation of the phospholipid bilayer. Indeed, the same MD simulation also supports this second mechanism. In the previous paper,²⁷ which focused on the behavior of the DPPC/melittin components of this complex MD simulation, it was found that melittin induces disorder in the phospholipid bilayer (especially of the lower "intracellular" layer which hosts melittin's loose N-terminus). Melittin-induced structural perturbations were also observed in the MD simulation of Berneche *et al.*²⁵ Experimental evidence for the role of structural perturbations in inducing lysis is given, for example, by the observation that membrane deformation plays an important role in ion transport across membranes.⁶⁶

Thus, the MD simulation reported here indicates that both mechanisms of melittin-induced lysis can occur concur-

rently. Melittin's effect on the membrane system is clearly multifaceted. It modifies the orientation of water molecules at, and near, the interface region, it induces the formation of water pores, and at the same time disrupts the structure of the membrane by inducing disorder in the phospholipid layers.

V. CONCLUSIONS

In this paper we analyzed a large molecular dynamics simulation of a DPPC membrane with an embedded peptide, the bee venom toxin melittin, elucidating the effect of the peptide on the surrounding water molecules. It was found that melittin has a profound effect on the behavior of the water molecules at the membrane/water interface. The embedded peptide modifies the orientation of the water dipoles at, and near, that interface and at the same time induces water penetration into the hydrophobic core of the bilayer. Most interesting is the finding that the peptide facilitates the formation of transmembrane water pores by steering water penetration from both sides of the bilayer. Taking advantage of the detailed insights offered by the computer simulation, we conclude that residue Lys-7 is the key functional group inducing water penetration from the extracellular side of the membrane, and the protonated N-terminus is the functional group inducing water penetration from the intracellular side. These two membrane-embedded positively charged residues have dipole moments directed each at the corresponding membrane/water interface. The simulation indicates that the initial phase of pore formation is very fast, taking place on the time scale of 200 ps. The simulation results and the suggested mechanism for melittin-induced lysis is supported by a large body of experimental observations.

The present MD simulation indicates that at least two of the proposed mechanisms for melittin-induced lysis: both pore formation and membrane perturbation, occur concurrently upon introduction of melittin into the system. Melittin modifies the orientation of water molecules at and near the interface region, induces the formation of water pores, and disrupts the order in the phospholipid layers all at the same time.

ACKNOWLEDGMENTS

The authors are grateful to R. W. Pastor and S. E. Feller for allowing them to use their equilibrated model of a pure DPPC bilayer, as well as for their helpful advice. This study was supported in part by a grant from the Israel Science Foundation and by a grant from the Israeli Interuniversity Supercomputing Center.

¹D. P. Tieleman, S. J. Marrink, and H. J. C. Berendsen, *Biochim. Biophys. Acta* **1331**, 235 (1997).

²K. Gawrisch *et al.*, *Biophys. J.* **61**, 1213 (1992).

³T. R. Stouch, H. E. Alper, and D. Bassolino-Klimas, *Supercomputing Applications High Performance Computing* **8**, 6 (1994).

⁴P. van der Ploeg and H. J. C. Berendsen, *J. Chem. Phys.* **76**, 3271 (1982).

⁵H. Heller, M. Schaefer, and K. Schulten, *J. Phys. Chem.* **97**, 8343 (1993).

⁶R. W. Pastor, *Curr. Opin. Struct. Biol.* **4**, 486 (1994).

⁷K. V. Damodaran and K. M. Merz, Jr., in *Reviews in Computational Chemistry*, edited by K. B. Lipkowitz and D. B. Boyd (VCH, New York, 1994).

⁸H. E. Alper and T. R. Stouch, *J. Phys. Chem.* **99**, 5724 (1995).

- ⁹S.-W. Chiu, M. Clark, S. Subramanian, H. L. Scott, and E. Jakobsson, *Biophys. J.* **69**, 1230 (1995).
- ¹⁰S. J. Marrink, R. M. Sok, and H. J. C. Berendsen, *J. Chem. Phys.* **104**, 9090 (1996).
- ¹¹J. J. Lopez Cascales, J. Garcia de la Torre, S. J. Marrink, and H. J. C. Berendsen, *J. Chem. Phys.* **104**, 2713 (1996).
- ¹²D. P. Tieleman and H. J. C. Berendsen, *J. Chem. Phys.* **105**, 4871 (1996).
- ¹³S. E. Feller, R. M. Venable, and R. W. Pastor, *Langmuir* **13**, 6555 (1997).
- ¹⁴O. Berger, O. Edholm, and F. Jahnig, *Biophys. J.* **72**, 2002 (1997).
- ¹⁵S. J. Marrink, O. Berger, P. Tieleman, and F. Jahnig, *Biophys. J.* **74**, 931 (1998).
- ¹⁶H. E. Alper, D. Bassolino-Klimas, and T. R. Stouch, *J. Chem. Phys.* **99**, 5547 (1993).
- ¹⁷S. J. Marrink, D. P. Tieleman, A. R. van Buuren, and H. J. C. Berendsen, *Faraday Discuss.* **103**, 191 (1996).
- ¹⁸F. Zhou and K. Schulten, *J. Phys. Chem.* **99**, 2194 (1995).
- ¹⁹S. A. Simon and T. J. McIntosh, *Proc. Natl. Acad. Sci. USA* **86**, 9263 (1989).
- ²⁰K. V. Damodaran, K. M. Merz, Jr., and B. P. Gaber, *Biophys. J.* **69**, 1299 (1995).
- ²¹T. B. Woolf and B. Roux, *Proteins* **24**, 92 (1996).
- ²²K. Belohorcova, J. H. Davis, T. B. Woolf, and B. Roux, *Biophys. J.* **73**, 3039 (1997).
- ²³T. B. Woolf, *Biophys. J.* **74**, 115 (1998).
- ²⁴L. Y. Shen, D. Bassolino, and T. Stouch, *Biophys. J.* **73**, 3 (1997).
- ²⁵S. Berneche, M. Nina, and B. Roux, *Biophys. J.* **75**, 1603 (1998).
- ²⁶D. P. Tieleman, M. S. P. Sansom, and H. J. C. Berendsen, *Biophys. J.* **76**, 40 (1999).
- ²⁷M. Bachar and O. M. Becker, *Biophys. J.* (in print).
- ²⁸D. P. Tieleman and H. J. C. Berendsen, *Biophys. J.* **74**, 2786 (1998).
- ²⁹T. C. Terwilliger and D. Eisenberg, *J. Biol. Chem.* **257**, 6016 (1982).
- ³⁰C. E. Dempsey, *Biochim. Biophys. Acta* **1031**, 143 (1990).
- ³¹H. Vogel and F. Jahnig, *Biophys. J.* **50**, 573 (1986).
- ³²A. Pastore, T. S. Harvey, C. E. Dempsey, and I. D. Campbell, *Eur. Biophys. J.* **16**, 363 (1989).
- ³³R. Bazzo *et al.*, *Eur. J. Biochem.* **173**, 4 (1988).
- ³⁴M. Milik and J. Skolnick, *Proteins: Struct., Funct., Genet.* **15**, 10 (1993).
- ³⁵H. Vogel, *Biochemistry* **26**, 4562 (1987).
- ³⁶E. Habermann and H. Kowallek, *Hoppe-Seyler's Z. Physiol. Chem.* **351**, 884 (1970).
- ³⁷R. Manjunatha-Kini and H. J. Evans, *Int. J. Pept. Protein Res.* **34**, 277 (1989).
- ³⁸V. S. Gevod and K. S. Birdi, *Biophys. J.* **45**, 1079 (1984).
- ³⁹P. Ducarme, M. Rahman, and B. Brasseur, *Proteins* **30**, 357 (1998).
- ⁴⁰M. T. Tosteson, S. J. Holmes, M. Razin, and D. C. Tosteson, *J. Membr. Biol.* **87**, 35 (1985).
- ⁴¹W. F. DeGrado, G. F. Musso, M. Lieber, E. T. Kaiser, and F. J. Kezdy, *Biophys. J.* **37**, 329 (1982).
- ⁴²E. J. Dufourc, I. C. P. Smith, and J. Dufourcq, *Biochemistry* **25**, 6448 (1986).
- ⁴³C. Ho and C. D. Stubbs, *Biophys. J.* **63**, 897 (1992).
- ⁴⁴R. E. Jacobs and S. H. White, *Biochemistry* **28**, 3421 (1989).
- ⁴⁵S. J. Marrink and H. J. C. Berendsen, *J. Phys. Chem.* **98**, 4155 (1994).
- ⁴⁶A. J. Weaver, M. D. Kemple, J. W. Brauner, R. Mendelsohn, and F. G. Prendergast, *Biochemistry* **31**, 1301 (1992).
- ⁴⁷J. P. Bradshaw, C. E. Dempsey, and A. Watts, *Mol. Membr. Biol.* **11**, 79 (1994).
- ⁴⁸M. Monette and M. Lafleur, *Biophys. J.* **68**, 187 (1995).
- ⁴⁹T. D. Bradrick, A. Philippetis, and S. Georghiou, *Biophys. J.* **69**, 1999 (1995).
- ⁵⁰S. E. Feller and R. W. Pastor, *Biophys. J.* **71**, 1350 (1996).
- ⁵¹M. Schlenkerich, J. Brickman, A. D. MacKerell, and M. Karplus, in *Biological Membranes: A Molecular Perspective from Computation and Experiment*, edited by K. Merz and B. Roux (Birkhauser, Boston, MA, 1996).
- ⁵²A. MacKerell *et al.*, *J. Phys. Chem. B* **102**, 3586 (1998).
- ⁵³J. F. Nagle *et al.*, *Biophys. J.* **70**, 1419 (1996).
- ⁵⁴B. R. Brooks *et al.*, *J. Comput. Chem.* **4**, 187 (1983).
- ⁵⁵S. E. Feller, R. W. Pastor, A. Rojnackarin, S. Bogusz, and B. R. Brooks, *J. Phys. Chem.* **100**, 17011 (1996).
- ⁵⁶S. E. Feller, Y. Zhang, R. W. Pastor, and B. R. Brooks, *J. Chem. Phys.* **103**, 4613 (1995).
- ⁵⁷R. Koynova and M. Caffrey, *Biochim. Biophys. Acta* **1376**, 91 (1998).
- ⁵⁸T. B. Woolf, *Biophys. J.* **73**, 2376 (1997).
- ⁵⁹H. Frischleder and G. Peinel, *Chin. Phys. Lipids* **30**, 121 (1982).
- ⁶⁰S. J. Marrink, F. Jahnig, and H. J. C. Berendsen, *Biophys. J.* **71**, 632 (1996).
- ⁶¹M. T. Tosteson and D. C. Tosteson, *Biophys. J.* **36**, 109 (1981).
- ⁶²M. J. Clague and R. J. Cherry, *Biochem. J.* **252**, 791 (1988).
- ⁶³A. J. Weaver, M. D. Kemple, and F. G. Prendergast, *Biochemistry* **28**, 8614 (1989).
- ⁶⁴S. E. Blondelle and R. A. Houghten, *Biochemistry* **30**, 4671 (1991).
- ⁶⁵S. E. Blondelle and R. A. Houghten, *Pept. Res.* **4**, 12 (1991).
- ⁶⁶M. A. Wilson and A. Pohorille, *J. Am. Chem. Soc.* **118**, 6580 (1996).